JACS
JOURNAL OF THE AMERICAN CHEMICAL SOCIETY

Communication

pubs.acs.org/JACS

A Chiral Porous Metal–Organic Framework for Highly Sensitive and Enantioselective Fluorescence Sensing of Amino Alcohols

Marcela M. Wanderley,[†] Cheng Wang,[†] Chuan-De Wu, and Wenbin Lin*

Department of Chemistry, CB#3290, University of North Carolina, Chapel Hill, North Carolina 27599, United States

Supporting Information

ABSTRACT: A highly porous and fluorescent metal–organic framework (MOF), **1**, was built from a chiral tetracarboxylate bridging ligand derived from 1,1′-bi-2-naphthol (BINOL) and a cadmium carboxylate infinite-chain secondary building unit. The fluorescence of **1** can be effectively quenched by amino alcohols via H-bonding with the binaphthol moieties decorating the MOF, leading to a remarkable chiral sensor for amino alcohols with greatly enhanced sensitivity and enantioselectivity over BINOL-based homogeneous systems. The higher detection sensitivity of **1** is due to a preconcentration effect by which the analytes are absorbed and concentrated inside the MOF channels, whereas the higher enantioselectivity of **1** is believed to result from enhanced chiral discrimination owing to the cavity confinement effect and the conformational rigidity of the BINOL groups in the framework. **1** was quenched by four chiral amino alcohols with unprecedentedly high Stern–Volmer constants of 490–31200 M^{-1} and enantioselectivity ratios of 1.17–3.12.

As a new class of crystalline porous materials, metal–organic frameworks (MOFs) have attracted a great deal of interest, mainly because they can be rationally designed and functionalized at the molecular level.[1] The exceptionally high porosity of MOFs allows ready access to their functional building blocks, enabling applications in diverse areas such as gas storage and separation,[2] drug delivery,[3] bioimaging,[4] catalysis,[5] and chemical sensing.[6] We are interested in developing MOFs as chemical sensors, not only to take advantage of the ready analyte access to the sensing sites in a highly porous platform but also because of the ease of interfacing MOFs with solid-state devices. It is well-established that porous materials, including MOFs, can take up molecules/ions into their internal volumes with much higher internal concentrations than in the external medium as a result of preferential interactions between the molecules/ions and the pore surfaces.[5a,7] We surmised that such a preconcentration effect can be utilized to enhance the sensitivity in chemical sensing.[8] In addition, chiral MOFs with suitable recognition sites can allow chiral sensing with greater stereoselectivity as a result of the confinement effect[9] exerted by the MOF framework and the conformational rigidity of the sensing sites.[10]

The inability to determine rapidly the enantiomeric makeup of products currently creates a bottleneck for high-throughput screening of enantioselective reactions.[11] Chiral fluorescence sensors are among the most logical choices for high-throughput determinations of enantiomeric excesses (ee's) of chiral compounds. Optically pure 1,1′-bi-2-naphthol (BINOL) derivatives have been extensively explored as enantioselective fluorescence sensors for a variety of chiral compounds with amino, hydroxyl, and carboxylate functionalities that can form hydrogen bonds with the two hydroxyl groups of BINOL.[12a] For example, Irie and co-workers first reported the enantioselective fluorescence quenching of BINOL by optically active amines. The decrease in the fluorescence signal depended on the quencher and solvent environment; the fluorescence quenching followed Stern–Volmer (SV) behavior with a SV constant (K_{SV}) of up to 50 M^{-1} in acetonitrile and an enantioselective $K_{SV}(S)/K_{SV}(R)$ ratio of up to 4.0 in *n*-hexane.[13] Pu and co-workers used dendritic antenna structures to amplify the fluorescence response of BINOL for the detection of amino alcohols.[12] A phenylene–ethynylene-based dendrimer underwent enantioselective quenching by amino alcohols, including valinol, leucinol, and phenylalaninol, with $K_{SV}(S)/K_{SV}(R)$ = 1.10–1.27 and a maximum K_{SV} of 560 M^{-1} in a benzene/hexane mixture.[12b] Pu and co-workers have also developed fluorescence enhancement sensors in which the analytes form hydrogen bonds with a built-in quencher in the molecule to release the fluorescent BINOL core and give enhanced fluorescence signals.[14a,b] The BINOL moiety has been incorporated into molecular squares by Lee and Lin[14c] and Pu and co-workers[14d,e] to afford better-defined chiral pockets for enhanced enantioselectivity toward amino alcohol quenching relative to the monomeric building blocks. Here we report the chiral porous MOF $[Cd_2(\mathbf{L})(H_2O)_2]\cdot 6.5DMF\cdot 3EtOH$ (**1**)

Scheme 1. Synthesis of 1 and Chemical Structures of the Amino Alcohol Quenchers

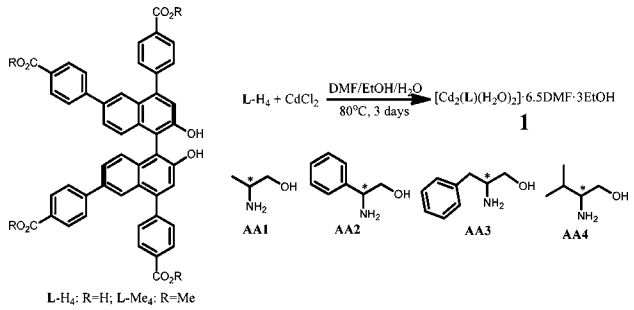

Received: March 2, 2012
Published: May 18, 2012

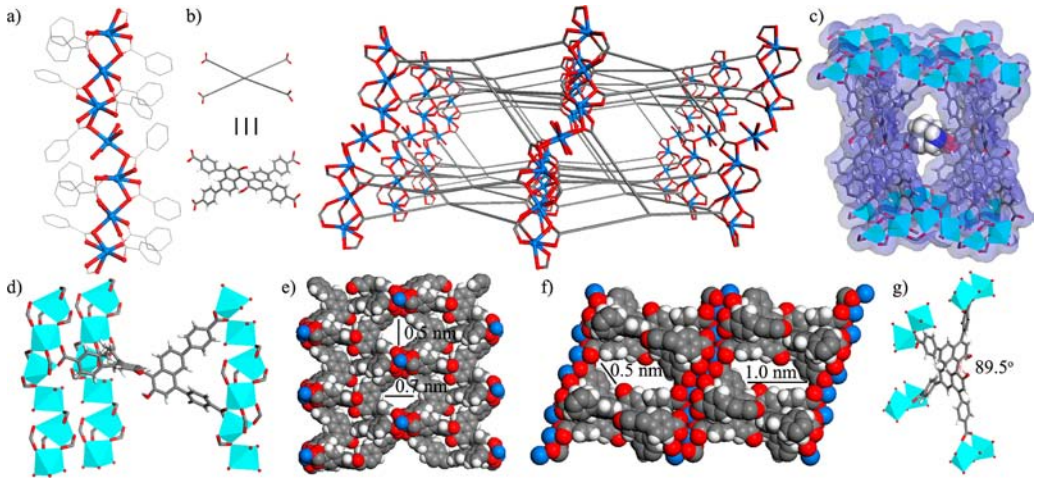

Figure 1. (a) Ball-and-stick model of an infinite 1D $[Cd_4(H_2O)_4(\mu_2\text{-}\eta^1,\eta^1\text{-}CO_2)_4(\mu_2\text{-}\eta^2,\eta^1\text{-}CO_2)_4]$ chain in **1**. (b) Ball-and-stick model showing the structure of **1** with the simplified **L** ligand, viewed along the [010] direction. (c) Analyte inside a MOF channel. The (*S*)-**AA4** molecule is represented by a space-filling model, while the framework is represented by a stick/polyhedron model. The Connolly surface of the framework, with a Connolly radius of 0.3 Å, is also shown in a semitransparent manner, indicating the interaction between the analyte molecule and the framework. (d) Coordination modes of the carboxylate groups of the **L** ligand, showing the bridging of three Cd centers that are further linked by the $Cd(H_2O)_4$ center to form the infinite chain as shown in (a). (e) Space-filling model of **1** viewed along the [001] direction. (f) Space-filling model of **1** viewed along the [010] direction. (g) The fixed dihedral angle between two naphthyl rings of the BINOL immobilized in **1** is believed to contribute to the enhanced enantioselectivity for fluorescence quenching by (*S*)-**AA4**. The colors in the ball-and-stick and space-filling presentations correspond to Cd (blue balls or cyan octahedra), C (gray), O (red), and H [white, omitted in (a) and (b)].

[**L**-H_4 = (*R*)-2,2′-dihydroxy-1,1′-binaphthyl-4,4′,6,6′-tetrakis(4-benzoic acid); DMF = *N*,*N*-dimethylformamide] as an enantioselective fluorescence sensor for amino alcohols. **1** is remarkably sensitive to amino alcohol quenchers, with SV constants as high as 31200 M^{-1} as a result of the preconcentration effect, and exhibits much-enhanced enantioselectivity toward the 2-amino-3-methyl-1-butanol quencher with a $K_{SV}(S)/K_{SV}(R)$ ratio of 3.12 because of the cavity confinement effect and conformational rigidity of the sensing site.

L-H_4 was synthesized according to a previously established procedure.[5a] A mixture of $CdCl_2$ and **L**-H_4 in a DMF/EtOH/H_2O solution was heated at 80 °C for 3 days to give light-yellow crystals of **1** (Scheme 1). Single-crystal X-ray diffraction (XRD) studies revealed that **1** crystallizes in the monoclinic *C*2 space group. There are three crystallographically independent Cd atoms in the structure, with Cd2 and Cd3 sitting on the twofold axis (with one-half occupancies). Both the Cd1 and Cd2 centers coordinate to six oxygen atoms of the bridging carboxylate groups of **L** ligands in a distorted octahedral geometry, whereas Cd3 coordinates to two oxygen atoms of bridging carboxylate groups in the axial positions and four water molecules in the equatorial positions to afford an octahedral geometry (Figure 1a). Cd1 and Cd2 are bridged by two μ_2-η^1,η^1-carboxylate groups and one μ_2-η^2,η^1-carboxylate group, while Cd3 is linked to two Cd1 centers through the μ_2-η^2,η^1-carboxylate groups. The Cd centers in **1** are thus linked by the bridging carboxylate groups to form one-dimensional (1D) chains having the formula $[Cd_4(H_2O)_4(\mu_2\text{-}\eta^1,\eta^1\text{-}CO_2)_4(\mu_2\text{-}\eta^2,\eta^1\text{-}CO_2)_4]$ along the [001] direction (Figure 1a). Each **L** ligand links three different 1D chains, leading to a 3D framework (Figure 1b,d). **1** is highly porous, with open channels having dimensions of 1.0 nm × 0.5 nm running along the [010] direction (Figure 1f) and open channels having dimensions of 0.7 nm × 0.5 nm running along the [001] direction (Figure 1e). PLATON calculations indicated the presence of 57.4% void space in **1**.

As expected, **1** is highly fluorescent, with an emission maximum at 440 nm and an emission lifetime of <3 ns. **1** was tested for fluorescence quenching by amino alcohols. Crystals of **1** were crushed by vigorous stirring with a magnetic stir bar and then suspended in acetonitrile to prepare a stock suspension of **1** (with the BINOL building block at a concentration of 8 μM). Aliquots containing different amounts of the *S* and *R* enantiomers of the amino alcohols 2-amino-1-propanol (**AA1**), 2-amino-2-phenylethanol (**AA2**), 2-amino-3-phenylpropanol (**AA3**), and 2-amino-3-methyl-1-butanol (**AA4**) (Scheme 1) were added to acetonitrile suspensions of **1** (3 mL). The fluorescence signals of the MOF suspensions in the presence of different amounts of amino alcohol quenchers were measured. The quenching of the fluorescence of **1** by the amino alcohols was highly efficient and followed SV behavior in the 0−4 μM concentration range (Figure 2a,b). A K_{SV} as high as 31200 M^{-1} was achieved with (*S*)-**AA2** (Table 1). Because of the short excited-state lifetime (<3 ns), low quencher concentration (0−4 μM), and low fluorophore concentration (8 μM), the collision probability during the lifetime of the fluorophore excited state was very low, and thus, the collisional quenching was negligible. Association of the quencher with BINOL in the ground state via hydrogen bonding followed by the formation of a poorly emissive proton-transfer-assisted charge-transfer excited state is proposed as the mechanism of the fluorescence quenching of BINOL. Time-resolved fluorescence measurements of **1** after addition of the quencher showed only a slight decrease in the decay rate [Figure S4.5 in the Supporting Information (SI)], consistent with the aforementioned hydrogen-bonding-based fluorescence quenching mechanism. **L**-Me_4 (Scheme 1) was used as a homogeneous control. The fluorescence of **L**-Me_4 was also quenched by the amino alcohols but with a much smaller K_{SV} than that of **1**.[15] The enhancement ratios of the MOF over the homogeneous control, $K_{SV}(\mathbf{1})/K_{SV}(\mathbf{L}\text{-}Me_4)$, were 289, 1038, 12, and 41 for (*S*)-**AA1**, -**AA2**, -**AA3**, and -**AA4**, respectively (Table 1). It is worth noting that **1** shows higher sensitivity toward amino

dx.doi.org/10.1021/ja302110d | *J. Am. Chem. Soc.* 2012, 134, 9050−9053

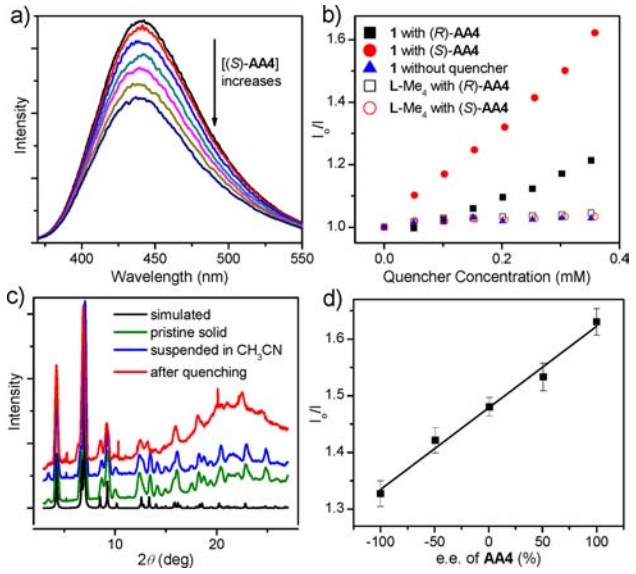

Figure 2. (a) Fluorescence emission spectra of **1** with increasing concentration of the (*S*)-**AA4** quencher in solution: 0, 0.05, 0.1, 0.15, 0.2, 0.26, and 0.31 mM (*S*)-**AA4** from top to bottom. (b) SV plots of the fluorescence emissions of **1** and **L**-Me$_4$ quenched by (*R*)- and (*S*)-**AA4**. The control experiment with MOF **1** was to test the photostability of **1** under the illumination conditions without addition of the quencher to the solution. (c) PXRD patterns of **1**: simulated (black), pristine (green), in acetonitrile (blue), and after the quenching experiment (red). (d) Plot of I_0/I vs the enantiomeric excess of **AA4** at a fixed concentration of 0.35 mM.

Table 1. SV Constants of 1 with Different (*S*)- and (*R*)-Amino Alcohol Quenchers

		Chiral amino alcohol quencher			
		AA1	**AA2**	**AA3**	**AA4**
1	$K_{SV}(S)$, M^{-1}	19400 ± 800	31000 ± 1000	680 ± 40	1660 ± 30
	$K_{SV}(R)$, M^{-1}	15500 ± 400	27000 ± 1000	490 ± 30	530 ± 40
	QR[a]	1.25 ± 0.06	1.17 ± 0.07	1.39 ± 0.03	3.12 ± 0.21
L-Me$_4$	$K_{SV}(S)$, M^{-1}	88 ± 4	35 ± 3	55 ± 2	48.9 ± 0.6
	$K_{SV}(R)$, M^{-1}	67 ± 1	30 ± 1	44 ± 1	40.5 ± 0.8
	QR[a]	1.31 ± 0.06	1.17 ± 0.11	1.25 ± 0.06	1.21 ± 0.03

[a]QR = $K_{SV}(S)/K_{SV}(R)$.

alcohol quenchers than all of the previously studied homogeneous BINOL-based systems.[12a] While all of the homogeneous systems require an analyte concentration in the millimolar range, **1** can sense amino alcohols at the micromolar concentration level. Using a ligand displacement strategy, Wolf and co-workers previously achieved the enantioselective sensing of amino alcohols at micromolar concentrations by either a UV−vis absorption or fluorescence quenching assay.[16]

We propose that the greatly enhanced detection sensitivity is due to preconcentration of the quencher within the channels of **1**. In essence, the solubility partition coefficient is such that the quencher molecules prefer the environment within the MOF to the acetonitrile solvent. To test this, we soaked crystals of **1** in a quencher solution having a known concentration. The concentration of the quencher in the supernatant was determined by gas chromatography (GC) analysis after the removal of **1** by centrifugation and derivatization of the amino alcohol with trifluoroacetic anhydride. **1** was dissolved in order to determine the amount of analyte it absorbed. GC analysis indicated that the concentration of the chiral amino alcohol within the channels of **1** was 4300 ± 600 and 5700 ± 900 times larger than that in the supernatant for (*R*)- and (*S*)-**AA4**, respectively.[17] The preconcentration factors were 6600 ± 1000 and 8500 ± 1300 for (*R*)- and (*S*)-**AA1**, respectively, and 5600 ± 1700 and 3500 ± 1000 for (*R*)- and (*S*)-**AA2**, respectively. Because of the significant errors associated with GC-derived preconcentration factors,[18] it was difficult to determine whether the analyte uptake process is enantioselective. Racemic **AA4** quencher was then used in the analyte uptake experiment. Chiral GC analysis indicated that **AA4** both inside the MOF and in the supernatant was racemic (with ee values of 0).[19] We thus conclude that the preconcentration step is not enantioselective.

1 shows high enantioselectivity toward chiral amino alcohols in fluorescence quenching. Here the enantioselectivity is expressed by the quenching ratio (QR), given by the ratio of SV constants for the (*S*)- and (*R*)-amino alcohols [i.e., QR = $K_{SV}(S)/K_{SV}(R)$]. The fluorescence of **1** was quenched by enantiomeric pairs of four chiral amino alcohols: **AA1**, **AA2**, **AA3**, and **AA4**. **1** showed the highest enantioselectivity for **AA4** (Table 1), with a QR of 3.12. In comparison, the homogeneous control (**L**-Me$_4$) gave a modest QR of 1.21. We believe that the steric confinement of the MOF cavity creates a more discriminating chiral environment for **AA4**, leading to a much-enhanced enantioselectivity (Figure 1c). The amino and hydroxyl groups on the **AA4** molecule form hydrogen bonds with a BINOL moiety, while the isopropyl group of the molecule can interact with the naphthyl rings of another BINOL on the other side of the cavity. This steric interaction reinforces the discrimination between the pair of enantiomers. The conformational rigidity of the immobilized BINOL may also contribute to the higher enantioselectivity (Figure 1g). The dihedral angle of the BINOL moiety immobilized in the MOF structure is fixed at 89.5°. Such rigidification of the sensing moiety reduces the non-enantioselective entropic term of the analyte association process and allows more stereospecific formation of the hydrogen-bonded complexes. Although the fluorescence of **1** is much more sensitive to the **AA1**, **AA2**, and **AA3** quenchers, the QR values for these three amino alcohols are essentially the same for **1** and **L**-Me$_4$.

We also tested the potential of using fluorescence quenching of **1** to quantify the ee of **AA4**. In this experiment, **1** was exposed to **AA4** (0.35 mM) with a variety of enantiomeric compositions, ranging from −100 to 100% ee with respect to the *S* enantiomer. The quenching response (I_0/I) was linearly correlated with the ee of **AA4** (Figure 2d). The ee of amino alcohol samples can thus be rapidly determined by a simple fluorescence quenching measurement with **1**.

The stability of **1** was carefully examined under the fluorescence quenching conditions. The fluorescence signals of both **L**-Me$_4$ and **1** decreased over time after long periods of illumination without the addition of amino alcohol. This was determined to be caused by photoreactivity of BINOL under the excitation beam of the fluorimeter (λ = 350 nm).[20] To minimize the influence of this photodecay on our measurements, all of the samples were carefully protected from light and were exposed to the excitation for only 3 s per measurement. Control experiments showed that the photoreactivity effects on this time scale were negligible in comparison with the change in signal caused by amino alcohol quenching (see the SI). Powder XRD (PXRD) patterns of a pristine sample of **1**, a crushed sample of **1** in acetonitrile (as is used for the experiments), and a crushed sample of **1** after exposure to amino alcohols and light all matched well with the PXRD pattern simulated from the X-ray structure of **1** (Figure

dx.doi.org/10.1021/ja302110d | J. Am. Chem. Soc. 2012, 134, 9050−9053

2c). This result supports the stability of **1** during the fluorescence sensing experiments.

In summary, a chiral porous MOF system for enantioselective fluorescence sensing of chiral amino alcohols has been successfully devised. **1** is a highly sensitive fluorescent sensor, with unprecedentedly high SV constants of up to 31200 M^{-1} as a result of preconcentration of the analyte inside the MOF cavities. **1** also shows impressive enantioselectivity, with an enantiomeric quenching ratio $[K_{SV}(S)/K_{SV}(R)]$ of 3.12 for 2-amino-3-methyl-1-butanol, presumably due to steric confinement by the MOF cavity as well as the conformational rigidity of the BINOL units. The amplified chiral discrimination of the analyte afforded by the confinement effect of the MOF cavities and the conformational rigidity of the sensing sites can be utilized to design MOF materials for other sensing applications.

■ ASSOCIATED CONTENT

Ⓢ Supporting Information

Experimental procedures and characterization data. This material is available free of charge via the Internet at http://pubs.acs.org.

■ AUTHOR INFORMATION

Corresponding Author

wlin@unc.edu

Author Contributions

†M.M.W. and C.W. contributed equally.

Notes

The authors declare no competing financial interest.

■ ACKNOWLEDGMENTS

We thank NSF (CHE-1111490) for financial support. C.W. acknowledges the UNC Department of Chemistry for an Ernest L. Eliel Fellowship.

■ REFERENCES

(1) (a) Férey, G.; Mellot-Draznieks, C.; Serre, C.; Millange, F. *Acc. Chem. Res.* **2005**, *38*, 217. (b) Kitagawa, S.; Kitaura, R.; Noro, S. *Angew. Chem., Int. Ed.* **2004**, *43*, 2334. (c) Evans, O. R.; Lin, W. *Acc. Chem. Res.* **2002**, *35*, 511. (d) Farha, O. K.; Hupp, J. T. *Acc. Chem. Res.* **2010**, *43*, 1166.

(2) (a) Dincă, M.; Long, J. R. *Angew. Chem., Int. Ed.* **2008**, *47*, 6766. (b) Rowsell, J. L.; Yaghi, O. M. *Angew. Chem., Int. Ed.* **2005**, *44*, 4670.

(3) (a) Lin, W.; Rieter, W. J.; Taylor, K. M. *Angew. Chem., Int. Ed.* **2009**, *48*, 650. (b) Rieter, W. J.; Pott, K. M.; Taylor, K. M.; Lin, W. *J. Am. Chem. Soc.* **2008**, *130*, 11584. (c) Horcajada, P.; et al. *Nat. Mater.* **2010**, *9*, 172.

(4) (a) deKrafft, K. E.; Xie, Z.; Cao, G.; Tran, S.; Ma, L.; Zhou, O. Z.; Lin, W. *Angew. Chem., Int. Ed.* **2009**, *48*, 9901. (b) Della Rocca, J.; Lin, W. B. *Eur. J. Inorg. Chem.* **2010**, 3725.

(5) (a) Ma, L.; Falkowski, J. M.; Abney, C.; Lin, W. *Nat. Chem.* **2010**, *2*, 838. (b) Ma, L.; Abney, C.; Lin, W. *Chem. Soc. Rev.* **2009**, *38*, 1248. (c) Lee, J.; Farha, O. K.; Roberts, J.; Scheidt, K. A.; Nguyen, S. T.; Hupp, J. T. *Chem. Soc. Rev.* **2009**, *38*, 1450.

(6) (a) Allendorf, M. D.; Houk, R. J.; Andruszkiewicz, L.; Talin, A. A.; Pikarsky, J.; Choudhury, A.; Gall, K. A.; Hesketh, P. J. *J. Am. Chem. Soc.* **2008**, *130*, 14404. (b) Chen, B.; Wang, L.; Xiao, Y.; Fronczek, F. R.; Xue, M.; Cui, Y.; Qian, G. *Angew. Chem., Int. Ed.* **2009**, *48*, 500. (c) Lan, A.; Li, K.; Wu, H.; Olson, D. H.; Emge, T. J.; Ki, W.; Hong, M.; Li, J. *Angew. Chem., Int. Ed.* **2009**, *48*, 2334. (d) Xie, Z.; Ma, L.; deKrafft, K. E.; Jin, A.; Lin, W. *J. Am. Chem. Soc.* **2010**, *132*, 922. (e) White, K. A.; Chengelis, D. A.; Gogick, K. A.; Stehman, J.; Rosi, N. L.; Petoud, S. *J. Am. Chem. Soc.* **2009**, *131*, 18069. (f) Shustova, N. B.; McCarthy, B. D.; Dincă, M. *J. Am. Chem. Soc.* **2011**, *133*, 20126.

(7) Wang, C.; Lin, W. *J. Am. Chem. Soc.* **2011**, *133*, 4232.

(8) (a) Gu, Z.-Y.; Wang, G.; Yan, X.-P. *Anal. Chem.* **2010**, *82*, 1365. (b) Shultz, A. M.; Farha, O. K.; Hupp, J. T.; Nguyen, S. T. *J. Am. Chem. Soc.* **2009**, *131*, 4204. (c) Kreno, L. E.; Hupp, J. T.; Van Duyne, R. P. *Anal. Chem.* **2010**, *82*, 8042. (d) Han, S.; Hermans, T. M.; Fuller, P. E.; Wei, Y.; Grzybowski, B. A. *Angew. Chem., Int. Ed.* **2012**, *51*, 2662.

(9) Jeong, K. S.; Go, Y. B.; Shin, S. M.; Lee, S. J.; Kim, J.; Yaghi, O. M.; Jeong, N. *Chem. Sci.* **2011**, *2*, 877.

(10) (a) Noyori, R.; Takaya, H. *Acc. Chem. Res.* **1990**, *23*, 345. (b) Yamakawa, M.; Noyori, R. *Organometallics* **1999**, *18*, 128.

(11) (a) Reetz, M. T. *Angew. Chem., Int. Ed.* **2001**, *40*, 284. (b) Traverse, J. F.; Snapper, M. L. *Drug Discovery Today* **2002**, *7*, 1002. (c) Tsukamoto, M.; Kagan, H. B. *Adv. Synth. Catal.* **2002**, *344*, 453. (d) Finn, M. G. *Chirality* **2002**, *14*, 534. (e) Leung, D.; Kang, S. O.; Anslyn, E. V. *Chem. Soc. Rev.* **2012**, *41*, 448.

(12) (a) Pu, L. *Acc. Chem. Res.* **2012**, *45*, 150. (b) Pugh, V. J.; Hu, Q.-S.; Pu, L. *Angew. Chem., Int. Ed.* **2000**, *39*, 3638. (c) Pugh, V. J.; Hu, Q.-S.; Zuo, X.; Lewis, F. D.; Pu, L. *J. Org. Chem.* **2001**, *66*, 6136. (d) Gong, L.-Z.; Hu, Q.-S.; Pu, L. *J. Org. Chem.* **2001**, *66*, 2358.

(13) (a) Yorozu, T.; Hayashi, K.; Irie, M. *J. Am. Chem. Soc.* **1981**, *103*, 5480. (b) Iwanek, W.; Mattay, J. *J. Photochem. Photobiol., A* **1992**, *67*, 209.

(14) (a) Chen, X.; Huang, Z.; Chen, S.-Y.; Li, K.; Yu, X.-Q.; Pu, L. *J. Am. Chem. Soc.* **2010**, *132*, 7297. (b) Lin, J.; Hu, Q.-S.; Xu, M.-H.; Pu, L. *J. Am. Chem. Soc.* **2002**, *124*, 2088. (c) Lee, S. J.; Lin, W. *J. Am. Chem. Soc.* **2002**, *124*, 4554. (d) Li, Z.-B.; Lin, J.; Pu, L. *Angew. Chem., Int. Ed.* **2005**, *44*, 1690. (e) Li, Z.-B.; Lin, J.; Zhang, H.-C.; Sabat, M.; Hyacinth, M.; Pu, L. *J. Org. Chem.* **2004**, *69*, 6284.

(15) **L**-Me_4 was used as a homogeneous control because of the poor solubility of **L**-H_4 in acetonitrile.

(16) (a) Mei, X.; Wolf, C. *J. Am. Chem. Soc.* **2006**, *128*, 13326. (b) Liu, S.; Pestano, J. P. C.; Wolf, C. *J. Org. Chem.* **2008**, *73*, 4267.

(17) Despite numerous attempts, **1** was not found to exhibit surface area as probed by nitrogen adsorption, presumably because of framework distortion upon solvent removal (see Figures S7.1,2). We have conclusively demonstrated that permanent porosity of evacuated MOFs (as probed by gas sorption experiments) is not a prerequisite for liquid-phase processes such as asymmetric catalysis and chiral sensing: Wang, C.; Zheng, M.; Lin, W. *J. Phys. Chem. Lett.* **2011**, *2*, 1701. The accessible void space inside the MOF channels (V_{free}) was calculated using PLATON. The amount of quencher absorbed by the MOF (n) was deterimined by GC analysis. The quencher concentration inside the MOF was calculated as n/V_{free}. See the SI for more details.

(18) The large experimental errors stemmed from a combination of the incomplete derivatization of the amino alcohols with trifluoroacetic anhydride (so different samples could have different yields) and the low TCD signals from rather dilute samples used in the fluorescence sensing studies and GC analyses. Attempts to concentrate the samples yielded inconsistent results because of evaporation of the amino alcohols and their derivatives.

(19) The experimental errors associated with the derivatization of the amino alcohols with trifluoroacetic anhydride and GC analysis were eliminated in the ee assay of the amino alcohols inside the MOF and in the supernatant. The relative signals in such measurements do not suffer from these experimental errors.

(20) (a) Flegel, M.; Lukeman, M.; Wan, P. *Can. J. Chem.* **2008**, *86*, 161. (b) Aein, N. B.; Wan, P. *J. Photochem. Photobiol., A* **2009**, *208*, 42. (c) Solntsev, K. M.; Bartolo, E. A.; Pan, G.; Muller, G.; Bommireddy, S.; Huppert, D.; Tolbert, L. M. *Isr. J. Chem.* **2009**, *49*, 227. (d) Nayak, M. K.; Wan, P. *Photochem. Photobiol. Sci.* **2008**, *7*, 1544.